Accepted Manuscript

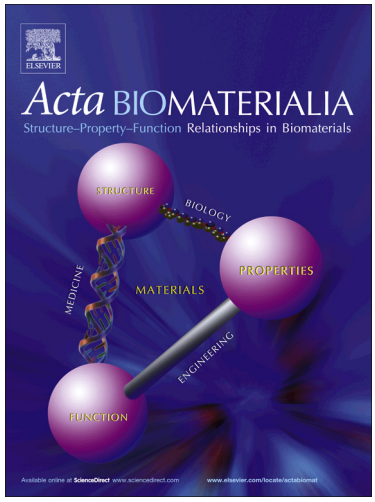

Choose Your Cell Model Wisely: The *In Vitro* Nanoneurotoxicity of Differentially Coated Iron Oxide Nanoparticles for Neural Cell Labeling

Freya Joris, Daniel Valdepérez, Beatriz Pelaz, Tianqiang Wang, Shareen H. Doak, Bella B. Manshian, Stefaan J. Soenen, Wolfgang J. Parak, Stefaan C. De Smedt, Koen Raemdonck

PII: S1742-7061(17)30224-6
DOI: http://dx.doi.org/10.1016/j.actbio.2017.03.053
Reference: ACTBIO 4821

To appear in: *Acta Biomaterialia*

Received Date: 25 November 2016
Revised Date: 27 March 2017
Accepted Date: 30 March 2017

Please cite this article as: Joris, F., Valdepérez, D., Pelaz, B., Wang, T., Doak, S.H., Manshian, B.B., Soenen, S.J., Parak, W.J., De Smedt, S.C., Raemdonck, K., Choose Your Cell Model Wisely: The *In Vitro* Nanoneurotoxicity of Differentially Coated Iron Oxide Nanoparticles for Neural Cell Labeling, *Acta Biomaterialia* (2017), doi: http://dx.doi.org/10.1016/j.actbio.2017.03.053

Choose Your Cell Model Wisely: The *In Vitro* Nanoneurotoxicity of Differentially Coated Iron Oxide Nanoparticles for Neural Cell Labeling.

Freya Joris[▲], *Daniel Valdepérez*[†], *Beatriz Pelaz*[†], *Tianqiang Wang*[†], *Shareen H. Doak*[§], *Bella B. Manshian*[◊], *Stefaan J. Soenen*[◊], *Wolfgang J. Parak*[†], *Stefaan C. De Smedt*[▲,1,*], *Koen Raemdonck*[▲,1]

[▲] Lab of General Biochemistry and Physical Pharmacy, Faculty of Pharmaceutical Sciences, Ghent University, Ottergemsesteenweg 460, B-9000 Ghent, Belgium.

[†] Philipps University of Marburg, Department of Physics, Renthof 7, D-35037 Marburg, Germany.

[§] Institute of Life Sciences, Swansea University Medical School, Singleton Park, Swansea, Wales, SA2 8PP, UK.

[◊] Biomedical MRI Unit/MoSAIC, Department of Medicine, KULeuven, Herestraat 49, B-3000 Leuven, Belgium.

[1] The authors contributed equally to this work

* Address correspondence to: stefaan.desmedt@ugent.be

Abstract

Currently, there is a large interest in the labeling of neural stem cells (NSCs) with iron oxide nanoparticles (IONPs) to allow MRI-guided detection after transplantation in regenerative medicine. For such biomedical applications, excluding nanotoxicity is key. Nanosafety is primarily evaluated *in vitro* where an immortalized or cancer cell line of murine origin is often applied, which is not necessarily an ideal cell model. Previous work revealed clear neurotoxic effects of PMA-coated IONPs in distinct cell types that could potentially be applied for nanosafety studies regarding neural cell labeling. Here, we aimed to assess if DMSA-coated IONPs could be regarded as a safer alternative for this purpose and how the cell model impacted our nanosafety optimization study. Hereto, we evaluated cytotoxicity, ROS production, calcium levels, mitochondrial homeostasis and cell morphology in six related neural cell types, namely neural stem cells, an immortalized cell line and a cancer cell line from human and murine origin. The cell lines mostly showed similar responses to both IONPs, which were frequently more pronounced for the PMA-IONPs. Of note, ROS and calcium levels showed opposite trends in the human and murine NSCs, indicating the importance of the species. Indeed, the human cell models were overall more sensitive than their murine counterpart. Despite the clear cell type-specific nanotoxicity profiles, our multiparametric approach revealed that the DMSA-IONPs outperformed the PMA-IONPs in terms of biocompatibility in each cell type. However, major cell type-dependent variations in the observed effects additionally warrant the use of relevant human cell models.

Keywords

IONP, DMSA, PMA, neural stem cell, cell line, multiparametric

Introduction

Nanotechnology yields numerous nanomaterials with interesting properties, which can be exploited in a plethora of possible applications. The biomedical field, for instance, aims to apply these materials to develop novel or improve existing diagnostic and/or therapeutic strategies.[1-4]

A category of inorganic nanoparticles (NPs) for biomedical use that has received much attention over the last two decades, are iron oxide (IO)NPs.[5] By creating nanosized iron oxide particles, the material acquires superparamagnetic properties, which allows its implementation in biomarker and pathogen detection assays[6-8], protein sequestration[8], cell sorting[9], drug delivery[10] and cancer treatment through hyperthermia.[5, 11] Importantly, IONPs can also be applied as contrast agents for magnetic resonance imaging (MRI).[12, 13] In this regard, FDA-approved dextran-coated IONPs (USA: Feridex®, EU: Endorem®) have been clinically applied for the MRI-guided detection of liver lesions and tumors, before the production was discontinued in 2009.[14, 15] This MRI susceptibility can furthermore be exploited for regenerative cell therapy, where stem cells are transplanted into damaged tissues to replace the latter or promote cell survival and tissue repair *via* the secretion of specific factors.[16, 17] To monitor the cell distribution and engraftment, such therapies require a non-invasive method to track the transplanted cells *in vivo*, which can be accomplished by *ex vivo* cell labeling prior to the transplantation.[16, 18]

In the context of regenerative medicine, there is a large interest in IONP labeling of neural stem cells before transplantation into the neural trauma site.[17, 19, 20] Since IONP with a diameter below 10 nm are typically applied for this purpose, we synthesized IONPs with a core diameter of ˜4 nm.[21] Overall, cell survival is an inherent drawback to this therapeutic modality and IONPs should persist inside the cells to allow long-term cell tracking, they may

not negatively affect cellular homeostasis.[18] Hence, IONP optimization in terms of nanosafety is of key importance. Previous work from our group on IONPs coated with poly(isobutylene-*alt*-maleic anhydride) grafted with dodecylamine (PMA) showed a disturbed cellular homeostasis at sublethal doses, making this construct less ideal for the labeling of neural cells.[22] Coating with the ligand 2,3-meso-dimercaptosuccinic acid (DMSA) could be a valuable alternative to improve the nanosafety profile. Indeed, DMSA is an FDA-approved chelator applied in case of lead intoxication and DMSA-IONPs show good biocompatibility both to neural cells *in vitro* and neural tissue *in vivo*.[23-25]

In general, many hazard identification studies are initially performed *in vitro* applying cell lines given their easy accessibility and applicability.[26-29] However, we and other groups have demonstrated that primary cells or stem cells often respond differently to NP exposure as compared to the cell line counterpart.[22, 30-32] In addition, murine cell types are regularly applied despite reported species-related variations in NP-induced effects, which impede the extrapolation of results towards possible human scenarios.[33-35] Although several groups investigated either the species or cell type associated diversity in NP-evoked responses,[36-38] such studies remain rare for neural cell types. Previous work from our group revealed cell type specific neurotoxicity profiles in response to PMA-IONPs.[22] Given the clear perturbation of cell homeostasis, the PMA-IONPs were considered less fit for neural stem cell labeling in the context of regenerative medicine. Hence, we set out to optimize the IONPs by applying a different coating. To investigate whether the cell type equally impacts nanosafety optimization studies we compared the nanosafety profile of DMSA-coated IONPs to the previously applied PMA-IONPs. Please note that the same PMA-IONP sample was applied as described in our previous work.[22] In short, we evaluated the cellular responses in neural cell types that could possibly be selected as an *in vitro* model for

neural stem cell labeling prior to transplantation in regenerative medicine, namely neural stem cells (NSCs), a neural immortalized (progenitor) cell line and neuroblastoma (cancerous) cell line from both humans and mice.[26-28] This setup will allow us to rationally guide the cell type selection for future nanosafety studies in the context of biomedical applications.

Materials & methods

1. IONP synthesis and characterization

IONPs were synthesized and coated with either the meso-2,3-dimercaptosuccinic acid (DMSA) ligand or the polymer poly(isobutylene-*alt*-maleic anhydride) grafted with dodecylamine (PMA) according to established protocols previously applied by our group.[22, 25, 39-41] Following synthesis, the core diameter was measured using transmission electron microscopy (TEM, Jeol JEM3010). UV/VIS absorption spectroscopy (Agilent 8453 UV-visible Spectroscopy System) was applied to evaluate the spectral characteristics, and the concentrations of the dispersions were determined *via* UV/VIS absorption spectroscopy and inductively coupled plasma mass spectrometry (ICP-MS, 7700 Series ICP-MS from Agilent Technologies). Finally, the hydrodynamic diameter and zeta-potential were measured using a Zetasizer Nano ZS (Malvern Instruments). Detailed information on the synthesis and characterization procedures is provided in the Supplementary Information.

2. Cell culture

The human NSCs (hNSCs [42]) were purchased from Invitrogen (Belgium). Both the murine NSCs (mNSCs [42]) and human progenitor cell line (ReNcell VM [43]) were obtained from Millipore (Belgium). Sigma (Belgium) provided the murine progenitor (C17.2 [44]) and

neuroblastoma (Neuro-2a [45]) cell line. Finally, the human neuroblastoma cell line (LA-N-2 [46]) was retrieved through the European Collection of Cell Cultures.

All cell types were cultured according to the manufacturers guidelines and kept at 37 °C in a humidified atmosphere completed with 5% CO_2. Every other day, cells received fresh cell medium until 80% confluence was reached and the cells were passaged. Hereto, the cells were detached using 0.05% trypsin–EDTA (Invitrogen, Belgium), centrifuged 4 minutes at 300 g and seeded at appropriate densities. Experiments were performed on cells with a passage number below 20. Detailed cell culture protocols are provided in the Supplementary Information.

3. Cytotoxicity

Cells were seeded in opaque 96-well plates at a density of 25000 cells/well and were allowed to settle overnight. The subsequent 24 hours, cells were exposed to 3.5, 7, 14, 35, 70 and 140 nM IONP dispersions. Subsequently, the CellTiter-GLO® assay (Promega, Belgium) was performed according to the manufacturer's instructions. Hereto, 100 µL of the assay buffer was added to each sample, plates were shaken during 2 minutes and following a 10-minute incubation, the signal was measured using a GloMax® 96 Luminometer (Promega, Belgium).

4. ROS and intracellular free calcium

Cells were seeded in 24-well plates at appropriate densities (Supplementary Information). The cells were allowed to settle overnight before being exposed to 7, 14, 35, 70 or 140 nM IONP dispersions for 24 hours. Notably, since the applied NP dispersion volume was adjusted according to the cell density, the NP number/volume cell medium/cell number remained equal in all experiments (Table S1).

After discarding the IONP containing medium, the cells were labelled with CellROX® green and Rhodamine-2 AM (Molecular Probes, Belgium) to allow visualization of reactive oxygen species (ROS) and free calcium present in the cytosol, respectively. Both were detected using the IN Cell analyser 2000 (GE Healthcare Life Sciences, Belgium) and the acquired data were analysed using in house developed protocols with the IN Cell Developer Toolbox software (GE Healthcare Life Sciences, Belgium). Detailed staining and analysis protocols are provided in the Supplementary Information.

5. Mitochondria and cell morphology

Cells were seeded at appropriate densities as described in the previous paragraph. The cells were allowed to settle overnight and were subsequently exposed to 3.5, 7, 14, 35 and 70 nM IONP dispersions. After a 24-hour incubation period, the NP dispersions were discarded and the mitochondria and cell cytoplasm were respectively labelled with Mitotracker® CMX-ROS Red and HCS CellMask™ Blue (both Molecular Probes, Belgium). Data were obtained with the IN Cell Analyzer 2000 and analysed with the IN Cell Developer Toolbox software. Detailed information on the staining procedure, data acquisition and data analysis is provided in the Supplementary Information.

6. Statistics

Cytotoxicity data are expressed as the mean ± standard error of the mean (SEM, n=3). IN Cell data are presented as the mean normalized against the untreated control ± SEM for two independent replicates, with a minimum of 10000 cells being analysed per replicate. Statistical analysis was performed using the 6th version of the GraphPad Prism software. Treated samples were compared with the untreated control by means of one-way ANOVA

combined with the post-hoc Dunnett test. Additionally, responses induced by the differently coated IONPs were compared with two-way ANOVA followed by the Bonferroni post-hoc test.

Results

1. IONP characterization

The core diameter (d_c) of the synthesized IONPs was quantified with transmission electron microscopy (TEM), which showed a mean value of 3.8 nm (Figure 1c & 1d). Next, the IONPs were coated with a ligand or polymer, respectively meso-2,3-dimercaptosuccinic acid (DMSA, Figure 1a) and poly-(isobutylene-*alt*-maleic) anhydride grafted with dodecylamine (PMA, Figure 1b).[22] As measured with dynamic light scattering, the hydrodynamic diameter in number distribution (d_h) was 11.83 ± 0.61 and 12.33 ± 0.75 nm with a polydispersity index of 0.185 and 0.308 for the DMSA- and PMA-coated IONPs, respectively. In addition, both IONPs showed a strong, negative charge of -55.5 ± 0.9 mV for the IONP-DMSA and -54 ± 2.2 mV for the IONP-PMA.[22] Further characterization in terms of the absorption spectra, molecular extinction coefficient, initial NP dispersion concentration and electrophoretic mobility is provided in the Supplementary Information (Tables S2 and S3, Figures S4 and S5).

2. Cytotoxicity

In a first set of cell-based experiments we evaluated the IONP-induced cell injury. Upon exposure to higher doses, several cell types experienced cell damage, which was most pronounced in the hNSCs (Figure 2). In contrast, the murine Neuro-2a neuroblastoma cell line was most resilient to IONP exposure, as only the highest dose of PMA-IONPs evoked a

minor, though significant, effect. In the majority of the cell types (the hNSCs, mNSCs and the murine C17.2 and Neuro-2a cell lines), the PMA-IONPs induced more severe effects than the DMSA-IONPs. However, in the ReNcell and LA-N-2 cell line, the opposite was true. Finally, when comparing the human cell types to their murine counterpart, the former appeared to be more sensitive, irrespective of the coating.

3. ROS production

To assess whether IONP exposure could affect the cell homeostasis at sublethal doses, we first looked into the effect of ROS production *via* staining with the CellROX® green probe.[47] This is especially important in neural cells since (i) ROS is a key player in the initiation and progression of several neurodegenerative disorders and (ii) neural cells are especially sensitive to oxidative stress given their high metabolic rate and low anti-oxidative capacity.[48] Three responses could be distinguished; an increase, a decline or a steady state (Figure 3). In case of the first two responses, the induced effects were IONP-concentration dependent. Similar to the cell damage, the observed changes in ROS levels were most pronounced in the NSCs. For instance, in the hNSCs the DMSA-coated IONPs evoked a three-fold ROS induction at the highest concentration tested, whereas a decline was induced by the IONP-PMA. Notably, exact opposite trends were obtained in the mNSCs, indicating species-specific effects. Likewise, in the human progenitor cell line (ReNcell), both IONPs caused ROS induction whereas a decline was seen in the murine counterpart (C17.2). In contrast, in both neuroblastoma cell lines only the PMA-coated IONPs significantly reduced ROS. Overall, the PMA-IONPs evoked more severe effects in the included cell lines but no general statements can be made on the interspecies variations.

4. Cytoplasmic calcium signal

Next, we evaluated the Ca^{2+} homeostasis in terms of the cytosolic free calcium concentration ($[Ca^{2+}]_c$) through Rhodamine-2 AM staining.[47] The latter is an important indicator of cell function, especially in neural cells, given its involvement in numerous intracellular processes (metabolic activity, gene expression, neurotransmitter release, cell proliferation and cell death, *etc.*).[49-52] Similar to the results on ROS production, we found either a concentration dependent decline or augmentation in $[Ca^{2+}]_c$ or no significant changes (Figure 4). In both NSCs and the C17.2 cell line, the differentially coated IONPs induced opposite effects. Where the PMA-IONPs caused an elevated $[Ca^{2+}]_c$ in the hNSCs and C17.2 cells, a significant decrease was noted for the DMSA-IONPs. Again, the opposite was true for the mNSCs. In the human progenitor cell line (ReNcell), Ca^{2+}-levels were significantly elevated by both IONPs and the PMA-IONPs, which once more evoked stronger responses. In the murine Neuro-2a cell line, both IONPs induced a significant decline, which was significantly greater for the IONP-DMSA. In the LA-N-2 cell line this response was only observed for the PMA-IONPs, as the DMSA-IONPs did not induce a significant effect. Here, less pronounced responses were detected in the murine NSCs and C17.2 cell line compared to their human counterparts.

5. Mitochondrial homeostasis

In turn, the mitochondria provide the bulk of the cellular energy, require Ca^{2+} signaling for their function, produce significant amounts of ROS and are associated with programmed cell death.[53, 54] In addition, the $\Delta_{\psi m}$ is a known effector in neurodegenerative disorders.[55] When the $\Delta_{\psi m}$ is compromised, the mitochondria fail to produce ATP and cytochrome C can be released, followed by the initiation of apoptosis.[53, 56] These organelles were labeled

with Mitotracker® CMX-ROS Red, which accumulates in the organelle based on the mitochondrial membrane potential ($\Delta\psi_m$). When the $\Delta\psi_m$ is compromised due to NPs directly interacting with the mitochondrial membrane or ROS-induced membrane damage, the dye can no longer accumulate and the mitochondrial signal area relative to the total cell area decreases.[57] Figure 5 shows the relative signal area to be reduced or unaffected by IONP exposure. The latter was true for both IONPs in the Neuro-2a cell line and the C17.2 cells exposed to DMSA-IONPs. In all other cases the IONPs significantly reduced the $\Delta\psi_m$. Notably, the ReNcells were most severely affected by both IONPs, followed by the hNSCs. Similar to the cytotoxicity observations, the human cell types were more sensitive to IONP exposure than the murine counterparts. On the whole, the onset of the effect occurred at lower doses for the IONP-PMA and effects were significantly more severe as compared to the DMSA-IONPs, except in the LA-N-2 neuroblastoma cells where no significant differences were detected between both IONPs.

6. Cell morphology

Following cell labeling with HCS CellMask™ Blue, cell morphology was evaluated in terms of cell area and cell circularity.[22] The latter is defined as a value between zero and one, with one representing a perfect sphere. Thus, a lower value corresponds to a more complex cell morphology whereas an increase due to IONP exposure points to cell rounding and loss of specific morphological features, such as neurite outgrowths.[22] Cell morphology is a convenient parameter to include in a multiparametric analysis, as cell death has specific morphological features whereas minor alterations to cytoskeleton building blocks can impair cell functions that require signaling *via* these components.[48, 50, 58, 59] Figure 6 reveals that the effect of the PMA-IONPs on cell morphology was overall more severe, with the

exception of the mNSCs. In the latter, both cell area and circularity were significantly affected by the lowest and highest dose of DMSA-IONPs and PMA-IONPs, respectively. Likewise, the hNSCs and ReNcells became smaller and more spherical starting from 14 nM PMA-IONPs, whereas DMSA-IONPs only significantly altered morphology at 70 nM. Cell circularity of the C17.2 cells was not significantly affected but the PMA-IONPs and DMSA-IONPs did reduce the cell area starting from the lowest and highest dose tested, respectively. The cell circularity of the Neuro-2a cells was elevated by both IONPs, while only the PMA-IONPs reduced the cell area at higher doses. Finally, since LA-N-2 cells tend to grow in clusters, the morphology was analyzed in terms of cluster area and cells per cluster. Here, the PMA-IONPs caused a significant concentration dependent decrease in both the average cluster area and number of cells per cluster at lower doses compared to the DMSA-IONPs (Figure 7).

Discussion

In this study, we evaluated the extent at which DMSA- and PMA-coated IONPs induced adverse effects in six neural cell types, namely NSCs, a progenitor cell line and a cancer cell line from murine and human origin. Please note that the same PMA-IONP sample was applied as in previous work, where we observed clear dose- and cell type-dependent neurotoxicity.[22] The specific aim of this work was to evaluate if such adverse effects could be similarly alleviated in the distinct cell types by applying a different coating strategy. The cell types were selected based on an important future application of the IONPs, i.e. neural cell labeling to allow MRI-guided *in vivo* cell tracking following transplantation in the context of regenerative cell therapy for neural lesions. Multiple studies regarding this topic apply various cell models without clearly specifying the species and or cell type (immortalized or

cancer cell line, primary cells, stem cells).[26-28] Since NP-evoked effects can differ widely amongst various cell models,[33, 35] we evaluated the impact of the cell model on nanosafety optimization studies. Hereto, we looked into the impact of both the cell type and species in one single study in contrast to previous reports focusing on a single variable.[34, 37, 38]

IONP characterization showed that DMSA- and PMA-IONPs had similar basic physicochemical properties, in line with previous reports.[22, 25, 39, 60] This was desirable as potentially distinct cell responses could be explained in terms of how the cell models interact with the NPs, rather than by the intrinsic physicochemical properties of the IONPs.

Overall, we found the DMSA-IONPs to evoke less extensive responses than the PMA-IONPs. In four out of six cell types DMSA-IONPs induced less cytotoxicity than the PMA-IONPs, as expected based on recent literature.[23-25] However, the observed toxicity for DMSA-IONPs was slightly more severe than anticipated, possibly due to the greater sensitivity of neural cells towards NP exposure in general.[16] Cell homeostasis was furthermore perturbed at sublethal IONP doses in nearly all combinations tested. In correspondence with previous reports, we witnessed unaffected, decreased or induced ROS levels, [55, 61, 62] which was more outspoken for the PMA-IONPs. The decreased ROS levels can be explained in terms of the intrinsic scavenging potential of intact IONPs or the cellular adaptation to the response of foreign materials.[63, 64] The steady state observed for DMSA-IONPs in the cancer cell lines can be attributed to the chelating capacity of DMSA, preventing leached iron ions from inducing ROS.[14, 23, 25] Still, the DMSA-IONPs were found to significantly induce ROS in the hNSCs and ReNcells, possibly indicating that the extent of ion leaching outweighed the DMSA chelating capacity or that ROS induction in part occurred through alternate mechanisms. Moreover, ROS induction is an acute event depending on the kinetics of NP

uptake, intracellular trafficking, the stability of the applied coating and ion leaching.[14, 65] Hence, variations in any of these processes could in part explain the distinct responses. Finally, variations between human and murine cell types may stem from differences in the anti-oxidative capacity, which was reported to be elevated in mice.[66] In addition, the DMSA-IONPs most often showed less pronounced responses on the level of the calcium and mitochondrial homeostasis and cell morphology. Since all responses can to a certain extent be correlated to ROS production,[65, 67] the chelating capacity of DMSA may in part be accountable for the improved nanosafety profile. However, additional elements may impact the safety profiles. For one, different coating materials will acquire different proteins at their surface. This differential protein corona can in turn influence the extent of NP uptake, the exploited uptake pathway(s) and subsequent cellular processing.[68] In addition, not all coating materials equally protect the IONP surface against the acidic pH and hydrolases in the lysosomes.[69] Of note, the coating itself may in turn be sensitive to lysosomal degradation and released degradation products can also affect the cell homeostasis.[70] Hence, further research will be required to unveil the exact mechanism behind the improved biocompatibility of DMSA-IONPs.

From the multiparametric data set in each cell type alone it would be concluded that the DMSA-IONPs are the preferred candidate for further optimization since they generally evoked less severe effects, regardless of the distinct culture medium composition for the different cell types. The cell media could potentially influence IONP uptake through an impact on the colloidal stability and the formation of a protein corona.[71, 72] Such variations in IONP uptake could certainly impact the evoked effects, although a linear relationship between the intracellular NP dose and the cytotoxicity is not always evident.[35] Hence, these parameters were not investigated in detail since we preferentially focused on

investigating how various cell models (*i.e.* the cell type and its optimal medium) respond to IONP exposure. Furthermore, adequate IONP uptake and colloidal stability were previously documented for the applied coating materials.[24, 47, 73] Nevertheless, further characterization of the protein corona and IONP uptake in the applied cell models would improve our understanding of the observed adverse events.[74]

Most importantly, a correct conclusion on the preferable IONP coating for the envisioned application could only be reached when a multiparametric approach was applied, as in rare cases the DMSA-IONPs more severely perturbed cell homeostasis. Overall, a distinct nanotoxicity profile was obtained in each applied cell model. The sensitivity of the cell model was furthermore clearly species-related, as human cell types were more sensitive towards DMSA-IONP-induced effects. Likewise, Zhang *et al.* found human macrophages to be more sensitive towards DMSA-IONPs than the murine alternative.[75] Secondly, the cell type was a major factor since for both the human and murine cell types the NSCs were found to be most sensitive towards both IONPs, whereas the cancer cell lines were most resilient. This is in agreement with the observation that tumor cells have several characteristics making them less prone to NP-induced effects, as cell transformation or immortalization is accompanied by phenotypical changes on the level of cell morphology, metabolic rate, proliferation rate, *etc*.[33, 76] Hence, intrinsic variations between cell types can at least in part be held accountable for the observed variations, as more elaborately described previously.[77] Finally, not all cell models showed a similar sensitivity on all evaluated end points. For instance, no significant differences could be detected in IONP-induced mitochondrial damage in the cancer cell lines, while this was true for all other cell types. Hence, nanosafety screenings to define suitable NPs for a certain application should be performed in a

multiparametric fashion evaluating sensitive and informative end points in sufficiently sensitive cell types.

To progress towards a clinical application, we should further investigate whether our cell labeling protocol allows sufficient IONP internalization to allow cell detection through MRI, as labeling parameters are reported to influence the MRI visibility.[78] IONP-labeled cells can generally be detected starting from 10-30 pg iron per cell.[79] However, the MRI signal is reported to decrease as a function of time due to IONP dilution through cell division and lysosomal degradation of the IONPs.[80-82] Thus, we should evaluate if sufficiently high intracellular IONP levels can be safely obtained with the sublethal IONP doses to ensure long-term cell tracking. Moreover, further testing would be required to establish the importance of the detected adverse events on long-term cell function and rule out delayed cytotoxicity, as this was previously observed for the DMSA-IONP labeling of primary neurons.[83] Based on our observations we suggest that NSCs are the preferred model for further investigation given the selected application. In preference the hNSCs should be applied since both NSCs showed opposite effects on the level of ROS and Ca^{2+} in response to DMSA-IONP labeling.

Conclusion

IONPs are of interest as MRI contrast agents for the labeling of transplanted neural stem cells (NSCs), albeit that nanotoxicity remains a concern. Cell-nanoparticle interactions of DMSA- and PMA-coated IONPs were investigated in human and murine NSC, neural progenitor and neuroblastoma cells. The overall nanosafety profile of the DMSA-IONPs was superior compared to the PMA-IONPs. Importantly, a multiparametric approach was required to reach this conclusion. In the cell lines we predominantly found both IONPs to

evoke similar responses. In contrast, clear interspecies variations were detected on ROS production and Ca^{2+} homeostasis in the NSCs, where both IONPs were found to evoke opposite effects. This is an important observation, as the hNSCs are considered to be the most representative model for the envisioned application. Thus, the DMSA-coating could not in all cell types equally alleviate the induced nanotoxicity compared to the PMA-IONPs. Overall, sufficiently sensitive cell lines can be applied when performing a multiparametric screening to define suitable candidates for a certain biomedical application. However, further thorough safety evaluations should be performed on a non-cancerous human cell model most closely resembling the target cell or tissue whenever possible.

Acknowledgements

F.J. is a doctoral fellow of the Agency for Innovation by Science and Technology in Flanders (IWT). S.J.S. is a postdoctoral fellow of the Research Foundation-Flanders (FWO). B.P. acknowledges the Alexander von Humboldt Foundation for a postdoctoral fellowship. We thank Sebastian Munck and Nicky Corthout (VIB Centre for Biology of Disease, Belgium) for use of the IN Cell Analyzer 2000 and IN Cell Developer Toolbox software. Additionally we wish to thank Karsten Kantner for the performed ICP measurements. Parts of this work were supported by DFG Germany (grant PA 794/25-1 to W.J.P.).

Conflict of interest

The authors declare that they have no competing interests.

References

[1] Canfarotta F, Piletsky SA. Engineered magnetic nanoparticles for biomedical applications. Advanced healthcare materials 2014;3:160-75.
[2] Kim T, Hyeon T. Applications of inorganic nanoparticles as therapeutic agents. Nanotechnology 2014;25:012001.
[3] Zarschler K, Rocks L, Licciardello N, Boselli L, Polo E, Garcia KP, De Cola L, Stephan H, Dawson KA. Ultrasmall inorganic nanoparticles: State-of-the-art and perspectives for biomedical applications. Nanomedicine : nanotechnology, biology, and medicine 2016;12:1663-701.
[4] Chan WCW, Udugama B, Kadhiresan P, Kim J, Mubareka S, Weiss PS, Park WJ. Patients, Here Comes More Nanotechnology. ACS nano 2016;10:8139-42.
[5] Wu W, Changzhong J, Roy VA. Recent progress in magnetic iron oxide-semiconductor composite nanomaterials as promising photocatalysts. Nanoscale 2015;7:38-58.
[6] Busquets MA, Sabate R, Estelrich J. Potential applications of magnetic particles to detect and treat Alzheimer's disease. Nanoscale research letters 2014;9:538.
[7] Wang EC, Wang AZ. Nanoparticles and their applications in cell and molecular biology. Integr Biol (Camb) 2014;6:9-26.
[8] Gu H, Xu K, Xu C, Xu B. Biofunctional magnetic nanoparticles for protein separation and pathogen detection. Chemical communications 2006:941-9.
[9] Majewski AP, Schallon A, Jerome V, Freitag R, Muller AH, Schmalz H. Dual-responsive magnetic core-shell nanoparticles for nonviral gene delivery and cell separation. Biomacromolecules 2012;13:857-66.
[10] Laurent S, Saei AA, Behzadi S, Panahifar A, Mahmoudi M. Superparamagnetic iron oxide nanoparticles for delivery of therapeutic agents: opportunities and challenges. Expert Opin Drug Deliv 2014;11:1449-70.
[11] Lim EK, Kim T, Paik S, Haam S, Huh YM, Lee K. Nanomaterials for theranostics: recent advances and future challenges. Chemical reviews 2015;115:327-94.
[12] Bakhtiary Z, Saei AA, Hajipour MJ, Raoufi M, Vermesh O, Mahmoudi M. Targeted superparamagnetic iron oxide nanoparticles for early detection of cancer: Possibilities and challenges. Nanomed-Nanotechnol 2016;12:287-307.
[13] Casula MF, Floris P, Innocenti C, Lascialfari A, Marinone M, Corti M, Sperling RA, Parak WJ, Sangregorio C. Magnetic Resonance Imaging Contrast Agents Based on Iron Oxide Superparamagnetic Ferrofluids. Chem Mater 2010;22:1739-48.
[14] Soenen SJ, Parak WJ, Rejman J, Manshian B. (Intra)cellular stability of inorganic nanoparticles: effects on cytotoxicity, particle functionality, and biomedical applications. Chemical reviews 2015;115:2109-35.
[15] Bobo D, Robinson KJ, Islam J, Thurecht KJ, Corrie SR. Nanoparticle-Based Medicines: A Review of FDA-Approved Materials and Clinical Trials to Date. Pharm Res 2016.
[16] Mahmoudi M, Hosseinkhani H, Hosseinkhani M, Boutry S, Simchi A, Journeay WS, Subramani K, Laurent S. Magnetic resonance imaging tracking of stem cells in vivo using iron oxide nanoparticles as a tool for the advancement of clinical regenerative medicine. Chemical reviews 2011;111:253-80.
[17] Levy M, Boulis N, Rao M, Svendsen CN. Regenerative cellular therapies for neurologic diseases. Brain Res 2016;1638:88-96.

[18] Taylor A, Wilson KM, Murray P, Fernig DG, Levy R. Long-term tracking of cells using inorganic nanoparticles as contrast agents: are we there yet? Chemical Society reviews 2012;41:2707-17.
[19] Chen CCV, Ku MC, Jayaseema DM, Lai JS, Hueng DY, Chang C. Simple SPION Incubation as an Efficient Intracellular Labeling Method for Tracking Neural Progenitor Cells Using MRI. PloS one 2013;8.
[20] Stoll EA. Advances toward regenerative medicine in the central nervous system: challenges in making stem cell therapy a viable clinical strategy. Mol Cell Ther 2014;2:12.
[21] Hahn MA, Singh AK, Sharma P, Brown SC, Moudgil BM. Nanoparticles as contrast agents for in-vivo bioimaging: current status and future perspectives. Analytical and bioanalytical chemistry 2011;399:3-27.
[22] Joris FV, D.; Pelaz, B.; Soenen, S.J.; Manshian, B.B.; Parak, W.J.; De Smedt, S.C.; Raemdonck, K. The impact of the species and cell type on the nanosafety profiles of iron oxide nanoparticles in neural cells. Journal of Nanobiotechnology2016.
[23] Vasconcelos Braz S, Monge-Fuentes V, Rodrigues da Silva J, Tomaz C, Tavares MC, Pereira Garcia M, Nair Bao S, Paulino Lozzi S, Bentes de Azevedo R. Morphological Analysis of Reticuloendothelial System in Capuchin Monkeys (Sapajus spp.) after Meso-2,3-Dimercaptosuccinic Acid (DMSA) Coated Magnetic Nanoparticles Administration. PloS one 2015;10:e0140233.
[24] Kim Y, Kong SD, Chen LH, Pisanic TR, Jin S, Shubayev VI. In vivo nanoneurotoxicity screening using oxidative stress and neuroinflammation paradigms. Nanomed-Nanotechnol 2013;9:1057-66.
[25] Mejias R, Gutierrez L, Salas G, Perez-Yague S, Zotes TM, Lazaro FJ, Morales MP, Barber DF. Long term biotransformation and toxicity of dimercaptosuccinic acid-coated magnetic nanoparticles support their use in biomedical applications. Journal of controlled release : official journal of the Controlled Release Society 2013;171:225-33.
[26] Shen WB, Vaccaro DE, Fishman PS, Groman EV, Yarowsky P. SIRB, sans iron oxide rhodamine B, a novel cross-linked dextran nanoparticle, labels human neuroprogenitor and SH-SY5Y neuroblastoma cells and serves as a USPIO cell labeling control. Contrast media & molecular imaging 2016;11:222-8.
[27] Egawa EY, Kitamura N, Nakai R, Arima Y, Iwata H. A DNA hybridization system for labeling of neural stem cells with SPIO nanoparticles for MRI monitoring post-transplantation. Biomaterials 2015;54:158-67.
[28] Neri M, Maderna C, Cavazzin C, Deidda-Vigoriti V, Politi LS, Scotti G, Marzola P, Sbarbati A, Vescovi AL, Gritti A. Efficient in vitro labeling of human neural precursor cells with superparamagnetic iron oxide particles: relevance for in vivo cell tracking. Stem Cells 2008;26:505-16.
[29] Joris F, Manshian BB, Peynshaert K, De Smedt SC, Braeckmans K, Soenen SJ. Assessing nanoparticle toxicity in cell-based assays: influence of cell culture parameters and optimized models for bridging the in vitro-in vivo gap. Chem Soc Rev 2013;42:8339-59.
[30] Bregoli L, Chiarini F, Gambarelli A, Sighinolfi G, Gatti AM, Santi P, Martelli AM, Cocco L. Toxicity of antimony trioxide nanoparticles on human hematopoietic progenitor cells and comparison to cell lines. Toxicology 2009;262:121-9.
[31] Feng W, Guo J, Huang H, Xia B, Liu H, Li J, Lin S, Li T, Liu J, Li H. Human normal bronchial epithelial cells: a novel in vitro cell model for toxicity evaluation. PloS one 2015;10:e0123520.

[32] Schlinkert P, Casals E, Boyles M, Tischler U, Hornig E, Tran N, Zhao JY, Himly M, Riediker M, Oostingh GJ, Puntes V, Duschl A. The oxidative potential of differently charged silver and gold nanoparticles on three human lung epithelial cell types. J Nanobiotechnol 2015;13.
[33] Luengo Y, Nardecchia S, Morales MP, Serrano MC. Different cell responses induced by exposure to maghemite nanoparticles. Nanoscale 2013;5:11428-37.
[34] Wang Y, Aker WG, Hwang HM, Yedjou CG, Yu H, Tchounwou PB. A study of the mechanism of in vitro cytotoxicity of metal oxide nanoparticles using catfish primary hepatocytes and human HepG2 cells. The Science of the total environment 2011;409:4753-62.
[35] Zhang H, Wang X, Wang M, Li L, Chang CH, Ji Z, Xia T, Nel AE. Mammalian Cells Exhibit a Range of Sensitivities to Silver Nanoparticles that are Partially Explicable by Variations in Antioxidant Defense and Metallothionein Expression. Small 2015;11:3797-805.
[36] Wilkinson KE, Palmberg L, Witasp E, Kupczyk M, Feliu N, Gerde P, Seisenbaeva GA, Fadeel B, Dahlen SE, Kessler VG. Solution-Engineered Palladium Nanoparticles: Model for Health Effect Studies of Automotive Particulate Pollution. ACS nano 2011;5:5312-24.
[37] Ekstrand-Hammarstrom B, Akfur CM, Andersson PO, Lejon C, Osterlund L, Bucht A. Human primary bronchial epithelial cells respond differently to titanium dioxide nanoparticles than the lung epithelial cell lines A549 and BEAS-2B. Nanotoxicology 2012;6:623-34.
[38] Kermanizadeh A, Gaiser BK, Ward MB, Stone V. Primary human hepatocytes versus hepatic cell line: assessing their suitability for in vitro nanotoxicology. Nanotoxicology 2013;7:1255-71.
[39] Sun S, Zeng H, Robinson DB, Raoux S, Rice PM, Wang SX, Li G. Monodisperse MFe2O4 (M = Fe, Co, Mn) nanoparticles. Journal of the American Chemical Society 2004;126:273-9.
[40] Lin CA, Sperling RA, Li JK, Yang TY, Li PY, Zanella M, Chang WH, Parak WJ. Design of an amphiphilic polymer for nanoparticle coating and functionalization. Small 2008;4:334-41.
[41] Schweiger C, Hartmann R, Zhang F, Parak WJ, Kissel TH, Rivera Gil P. Quantification of the internalization patterns of superparamagnetic iron oxide nanoparticles with opposite charge. J Nanobiotechnol 2012;10.
[42] Wu YY, Mujtaba T, Rao MS. Isolation of stem and precursor cells from fetal tissue. Methods Mol Biol 2002;198:29-40.
[43] Donato R, Miljan EA, Hines SJ, Aouabdi S, Pollock K, Patel S, Edwards FA, Sinden JD. Differential development of neuronal physiological responsiveness in two human neural stem cell lines. Bmc Neurosci 2007;8:36.
[44] Ryder EF, Snyder EY, Cepko CL. Establishment and Characterization of Multipotent Neural Cell-Lines Using Retrovirus Vector-Mediated Oncogene Transfer. J Neurobiol 1990;21:356-75.
[45] Klebe RJ, Ruddle RH. Neuroblastoma - Cell Culture Analysis of a Differentiating Stem Cell System. Journal of Cell Biology 1969;43:A69-&.
[46] Seeger RC, Rayner SA, Banerjee A, Chung H, Laug WE, Neustein HB, Benedict WF. Morphology, Growth, Chromosomal Pattern, and Fibrinolytic-Activity of 2 New Human Neuroblastoma Cell Lines. Cancer research 1977;37:1364-71.
[47] Manshian BB, Moyano DF, Corthout N, Munck S, Himmelreich U, Rotello VM, Soenen SJ. High-content imaging and gene expression analysis to study cell-nanomaterial interactions: the effect of surface hydrophobicity. Biomaterials 2014;35:9941-50.

[48] Wu YL, Putcha N, Ng KW, Leong DT, Lim CT, Loo SCJ, Chen XD. Biophysical Responses upon the Interaction of Nanomaterials with Cellular Interfaces. Accounts of chemical research 2013;46:782-91.
[49] Clapham DE. Calcium signaling. Cell 2007;131:1047-58.
[50] Zhivotovsky B, Orrenius S. Calcium and cell death mechanisms: a perspective from the cell death community. Cell calcium 2011;50:211-21.
[51] Jan E, Byrne SJ, Cuddihy M, Davies AM, Volkov Y, Gun'ko YK, Kotov NA. High-content screening as a universal tool for fingerprinting of cytotoxicity of nanoparticles. ACS nano 2008;2:928-38.
[52] Ariano P, Zamburlin P, Gilardino A, Mortera R, Onida B, Tomatis M, Ghiazza M, Fubini B, Lovisolo D. Interaction of spherical silica nanoparticles with neuronal cells: size-dependent toxicity and perturbation of calcium homeostasis. Small 2011;7:766-74.
[53] Brookes PS, Yoon Y, Robotham JL, Anders MW, Sheu SS. Calcium, ATP, and ROS: a mitochondrial love-hate triangle. American journal of physiology Cell physiology 2004;287:C817-33.
[54] Fulda S, Galluzzi L, Kroemer G. Targeting mitochondria for cancer therapy. Nature reviews Drug discovery 2010;9:447-64.
[55] Imam SZ, Lantz-McPeak SM, Cuevas E, Rosas-Hernandez H, Liachenko S, Zhang Y, Sarkar S, Ramu J, Robinson BL, Jones Y, Gough B, Paule MG, Ali SF, Binienda ZK. Iron Oxide Nanoparticles Induce Dopaminergic Damage: In vitro Pathways and In Vivo Imaging Reveals Mechanism of Neuronal Damage. Mol Neurobiol 2015;52:913-26.
[56] Gottlieb E, Armour SM, Harris MH, Thompson CB. Mitochondrial membrane potential regulates matrix configuration and cytochrome c release during apoptosis. Cell death and differentiation 2003;10:709-17.
[57] Pendergrass W, Wolf N, Poot M. Efficacy of MitoTracker Green and CMXrosamine to measure changes in mitochondrial membrane potentials in living cells and tissues. Cytometry Part A : the journal of the International Society for Analytical Cytology 2004;61:162-9.
[58] Buyukhatipoglu K, Clyne AM. Superparamagnetic iron oxide nanoparticles change endothelial cell morphology and mechanics via reactive oxygen species formation. Journal of biomedical materials research Part A 2011;96:186-95.
[59] Tay CY, Cai P, Setyawati MI, Fang W, Tan LP, Hong CH, Chen X, Leong DT. Nanoparticles strengthen intracellular tension and retard cellular migration. Nano letters 2014;14:83-8.
[60] Quarta A, Curcio A, Kakwere H, Pellegrino T. Polymer coated inorganic nanoparticles: tailoring the nanocrystal surface for designing nanoprobes with biological implications. Nanoscale 2012;4:3319-34.
[61] Harris G, Palosaari T, Magdolenova Z, Mennecozzi M, Gineste JM, Saavedra L, Milcamps A, Huk A, Collins AR, Dusinska M, Whelan M. Iron oxide nanoparticle toxicity testing using high-throughput analysis and high-content imaging. Nanotoxicology 2015;9 Suppl 1:87-94.
[62] Lindemann A, Ludtke-Buzug K, Fraderich BM, Grafe K, Pries R, Wollenberg B. Biological impact of superparamagnetic iron oxide nanoparticles for magnetic particle imaging of head and neck cancer cells. International journal of nanomedicine 2014;9:5025-40.
[63] Gao L, Zhuang J, Nie L, Zhang J, Zhang Y, Gu N, Wang T, Feng J, Yang D, Perrett S, Yan X. Intrinsic peroxidase-like activity of ferromagnetic nanoparticles. Nature nanotechnology 2007;2:577-83.

[64] Huang DM, Hsiao JK, Chen YC, Chien LY, Yao M, Chen YK, Ko BS, Hsu SC, Tai LA, Cheng HY, Wang SW, Yang CS, Chen YC. The promotion of human mesenchymal stem cell proliferation by superparamagnetic iron oxide nanoparticles. Biomaterials 2009;30:3645-51.
[65] Nel A, Xia T, Madler L, Li N. Toxic potential of materials at the nanolevel. Science 2006;311:622-7.
[66] Mukherjee SG, O'Claonadh N, Casey A, Chambers G. Comparative in vitro cytotoxicity study of silver nanoparticle on two mammalian cell lines. Toxicol in Vitro 2012;26:238-51.
[67] Soenen SJ, Manshian B, Montenegro JM, Amin F, Meermann B, Thiron T, Cornelissen M, Vanhaecke F, Doak S, Parak WJ, De Smedt S, Braeckmans K. Cytotoxic effects of gold nanoparticles: a multiparametric study. ACS nano 2012;6:5767-83.
[68] Maiorano G, Sabella S, Sorce B, Brunetti V, Malvindi MA, Cingolani R, Pompa PP. Effects of cell culture media on the dynamic formation of protein-nanoparticle complexes and influence on the cellular response. ACS nano 2010;4:7481-91.
[69] Soenen SJ, Himmelreich U, Nuytten N, De Cuyper M. Cytotoxic effects of iron oxide nanoparticles and implications for safety in cell labelling. Biomaterials 2011;32:195-205.
[70] Zhang L, Wang X, Zou J, Liu Y, Wang J. DMSA-Coated Iron Oxide Nanoparticles Greatly Affect the Expression of Genes Coding Cysteine-Rich Proteins by Their DMSA Coating. Chemical research in toxicology 2015;28:1961-74.
[71] Mahmoudi M, Laurent S, Shokrgozar MA, Hosseinkhani M. Toxicity evaluations of superparamagnetic iron oxide nanoparticles: cell "vision" versus physicochemical properties of nanoparticles. ACS nano 2011;5:7263-76.
[72] Rivera-Gil P, De Aberasturi DJ, Wulf V, Pelaz B, Del Pino P, Zhao YY, De La Fuente JM, De Larramendi IR, Rojo T, Liang XJ, Parak WJ. The Challenge To Relate the Physicochemical Properties of Colloidal Nanoparticles to Their Cytotoxicity. Accounts of chemical research 2013;46:743-9.
[73] Pisanic TR, 2nd, Blackwell JD, Shubayev VI, Finones RR, Jin S. Nanotoxicity of iron oxide nanoparticle internalization in growing neurons. Biomaterials 2007;28:2572-81.
[74] Maiolo D, Del Pino P, Metrangolo P, Parak WJ, Bombelli FB. Nanomedicine delivery: does protein corona route to the target or off road? Nanomedicine : nanotechnology, biology, and medicine 2015;10:3231-47.
[75] Zhang L, Wang X, Zou J, Liu Y, Wang J. Effects of an 11-nm DMSA-coated iron nanoparticle on the gene expression profile of two human cell lines, THP-1 and HepG2. J Nanobiotechnology 2015;13:3.
[76] Wang J, Fang X, Liang W. Pegylated phospholipid micelles induce endoplasmic reticulum-dependent apoptosis of cancer cells but not normal cells. ACS nano 2012;6:5018-30.
[77] Joris F, Valdeperez D, Pelaz B, Soenen SJ, Manshian BB, Parak WJ, De Smedt SC, Raemdonck K. The impact of species and cell type on the nanosafety profile of iron oxide nanoparticles in neural cells. J Nanobiotechnology 2016;14:69.
[78] Mathiasen AB, Hansen L, Friis T, Thomsen C, Bhakoo K, Kastrup J. Optimal labeling dose, labeling time, and magnetic resonance imaging detection limits of ultrasmall superparamagnetic iron-oxide nanoparticle labeled mesenchymal stromal cells. Stem Cells Int 2013;2013:353105.
[79] Korchinski DJ, Taha M, Yang R, Nathoo N, Dunn JF. Iron Oxide as an MRI Contrast Agent for Cell Tracking. Magn Reson Insights 2015;8:15-29.

[80] Soenen SJ, Vercauteren D, Braeckmans K, Noppe W, De Smedt S, De Cuyper M. Stable long-term intracellular labelling with fluorescently tagged cationic magnetoliposomes. Chembiochem 2009;10:257-67.
[81] Ruiz A, Gutierrez L, Caceres-Velez PR, Santos D, Chaves SB, Fascineli ML, Garcia MP, Azevedo RB, Morales MP. Biotransformation of magnetic nanoparticles as a function of coating in a rat model. Nanoscale 2015;7:16321-9.
[82] Petters C, Thiel K, Dringen R. Lysosomal iron liberation is responsible for the vulnerability of brain microglial cells to iron oxide nanoparticles: comparison with neurons and astrocytes. Nanotoxicology 2016;10:332-42.
[83] Petters C, Dringen R. Accumulation of iron oxide nanoparticles by cultured primary neurons. Neurochemistry international 2015;81:1-9.

Figure Captions

Figure 1: DMSA- and PMA-coated IONPs.
(a) DMSA-IONPs, (b) PMA-IONPs, (c) TEM image (scale bar corresponds to 20 nm) of the bare IONPs and (d) the corresponding size distribution histogram of the iron oxide cores $N(d_c)$.

Figure 2: Human cell types experience stronger dose dependent cytotoxicity.
Cytotoxicity as determined with the CellTiter GLO® assay following 24 hours exposure to DMSA- (black) and PMA-coated (white) IONPs. Statistical significance with regard to the untreated control is indicated when appropriate (* $p < 0.05$) in black for the DMSA-IONPs and grey for the PMA-coated IONPs. (NTC = not treated control)

Figure 3: IONP exposure affects ROS production.
The influence of 24 hours DMSA-IONP (black bars) and PMA-IONP (white bars) exposure on reactive oxygen species (ROS) production as detected with the CellROX® green probe, with the latter generally evoking stronger responses. When appropriate, statistical significance with respect to the untreated control is indicated in grey for the PMA-IONPs and in black for the DMSA-IONPs (* $p < 0.05$). (NTC = not treated control)

Figure 4: Increased or declined $[Ca^{2+}]_c$ by IONPs.
The cytosolic free calcium concentration ($[Ca^{2+}]_c$) was visualized with Rhod-2 AM following 24 hours exposure to DMSA-IONPs (black bars) and PMA-IONPs (white bars). Grey and black * represent significant alterations when compared to the untreated control (* $p < 0.05$) induced by respectively PMA-IONPs and DMSA-IONPs. (NTC = not treated control)

Figure 5: Mitochondria are more severely affected in the human cell types.
DMSA-IONP (black bars) and PMA-IONP (white bars) induced effects on mitochondrial homeostasis in terms of the relative mitochondrial area as visualized with Mitotracker® CMX-ROS. Statistical significance with regard to the untreated control is indicated when appropriate (* $p < 0.05$), in black for significant effects evoked by IONP-DMSA and in gray for the PMA-coated IONP. (NTC = not treated control)

Figure 6: DMSA-IONPs have a minor impact on cell morphology.
The effect on cell morphology of 24 hours exposure to DMSA-IONPs (top row) and PMA-IONPs (lower row) represented as changes in relative cell area (black bars) and cell circularity (blue lines). In general cell circularity is a more sensitive parameter and DMSA-IONPs induce least severe effects. Statistical significance with regard to the untreated control is indicated when appropriate in the corresponding color, black for cell area and blue for circularity (* $p < 0.05$). (NTC = not treated control)

Figure 7: LA-N-2 cell morphology is most affected by IONP-PMA exposure.
The effect of both IONPs on the LA-N-2 cell line in terms of the total cluster area (black bars) and cells per cluster (white bars). Grey and black * represent significant alterations when compared to the untreated control (* $p < 0.05$) for respectively cluster area and cells per cluster. (NTC = not treated control)

Choose Your Cell Model Wisely: The *In Vitro* Nanoneurotoxicity of Differentially Coated Iron Oxide Nanoparticles for Neural Cell Labeling.

Freya Joris[▲], *Daniel Valdepérez*[†], *Beatriz Pelaz*[†], *Tianqiang Wang*[†], *Shareen H. Doak*[§], *Bella B. Manshian*[◊], *Stefaan J. Soenen*[◊], *Wolfgang J. Parak*[†], *Stefaan C. De Smedt*[▲,1,*], *Koen Raemdonck*[▲,1]

[▲] Lab of General Biochemistry and Physical Pharmacy, Faculty of Pharmaceutical Sciences, Ghent University, Ottergemsesteenweg 460, B-9000 Ghent, Belgium.

[†] Philipps University of Marburg, Department of Physics, Renthof 7, D-35037 Marburg, Germany.

[§] Institute of Life Sciences, Swansea University Medical School, Singleton Park, Swansea, Wales, SA2 8PP, UK.

[◊] Biomedical MRI Unit/MoSAIC, Department of Medicine, KULeuven, Herestraat 49, B-3000 Leuven, Belgium.

[1] The authors contributed equally to this work

* Address correspondence to: stefaan.desmedt@ugent.be

FIGURES

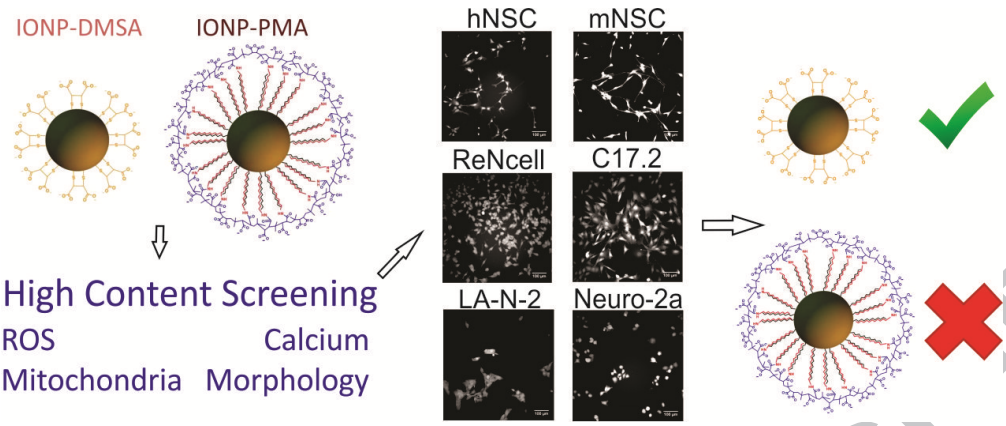

Graphical abstract

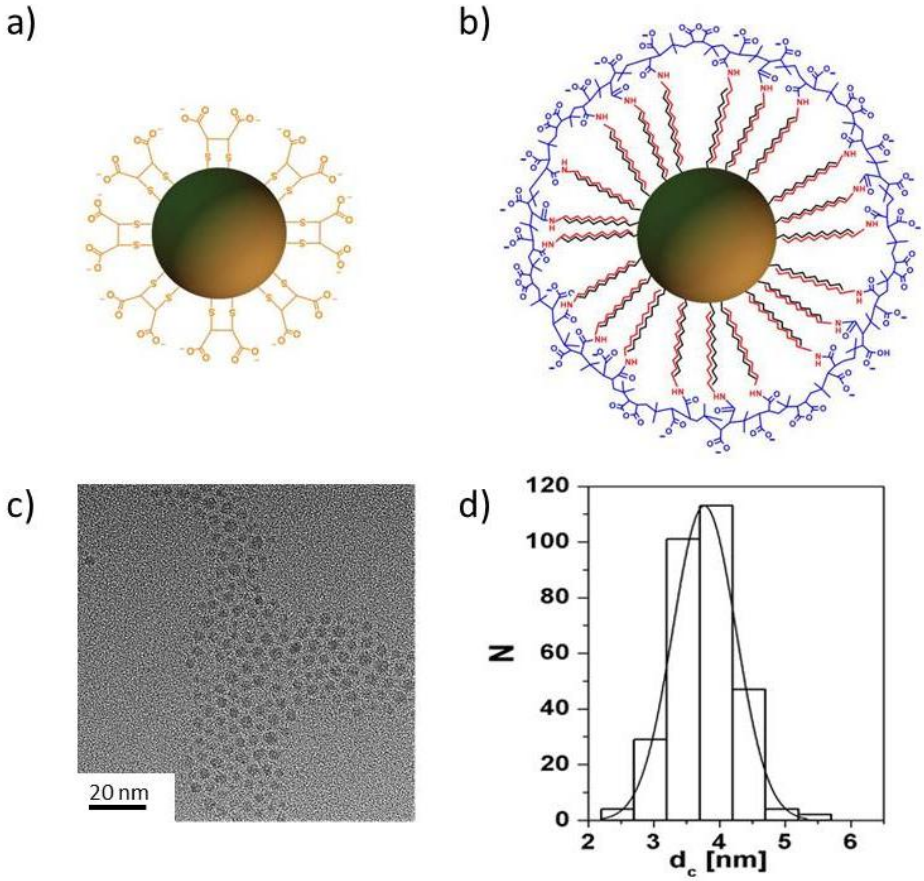

Figure 1: DMSA- and PMA-coated IONPs.

(a) DMSA-IONPs, (b) PMA-IONPs, (c) TEM image (scale bar corresponds to 20 nm) of the bare IONPs and (d) the corresponding size distribution histogram of the iron oxide cores $N(d_c)$.

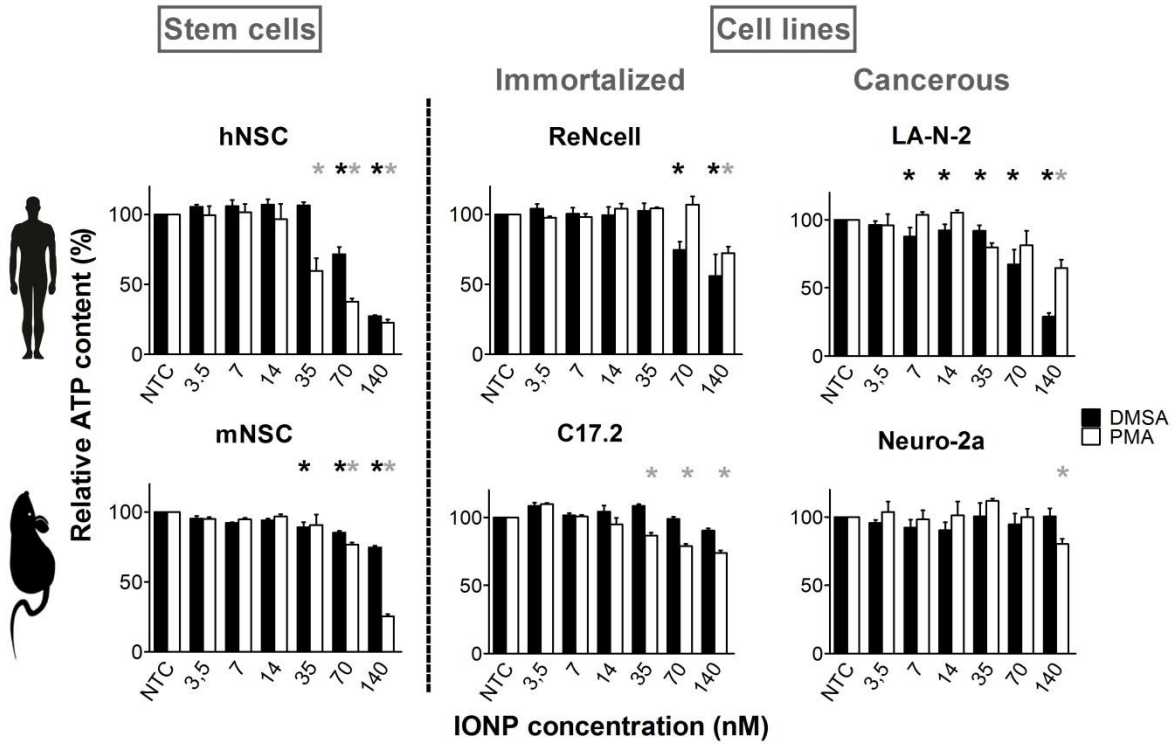

Figure 2: Human cell types experience stronger dose dependent acute cell damage.

Cytotoxicity as determined with the CellTiter GLO® assay following 24 hours exposure to DMSA- (black) and PMA-coated (white) IONPs. Statistical significance with regard to the untreated control is indicated when appropriate (* $p < 0.05$) in black for the DMSA-IONPs and grey for the PMA-coated IONPs. (NTC = not treated control)

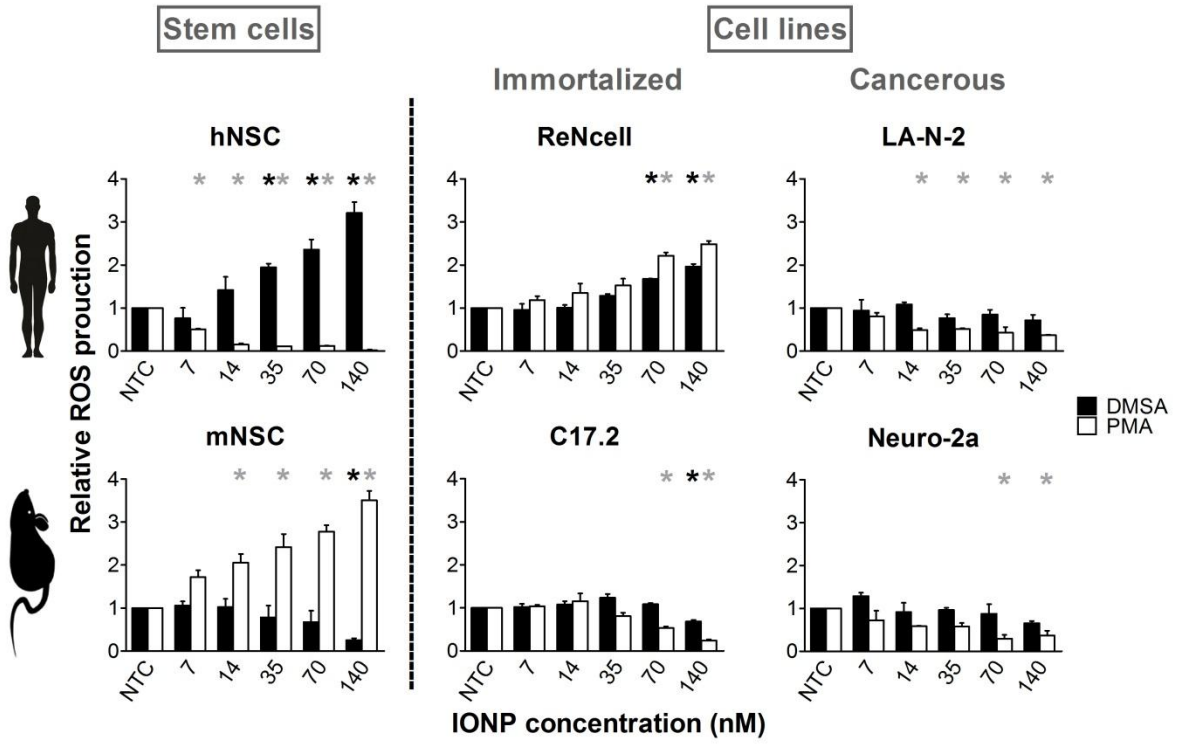

Figure 3: IONP exposure affects ROS production.

The influence of 24 hours DMSA-IONP (black bars) and PMA-IONP (white bars) exposure on reactive oxygen species (ROS) production as detected with the CellROX® green probe, with the latter generally evoking stronger responses. When appropriate, statistical significance with respect to the untreated control is indicated in grey for the PMA-IONPs and in black for the DMSA-IONPs (* $p < 0.05$). (NTC = not treated control)

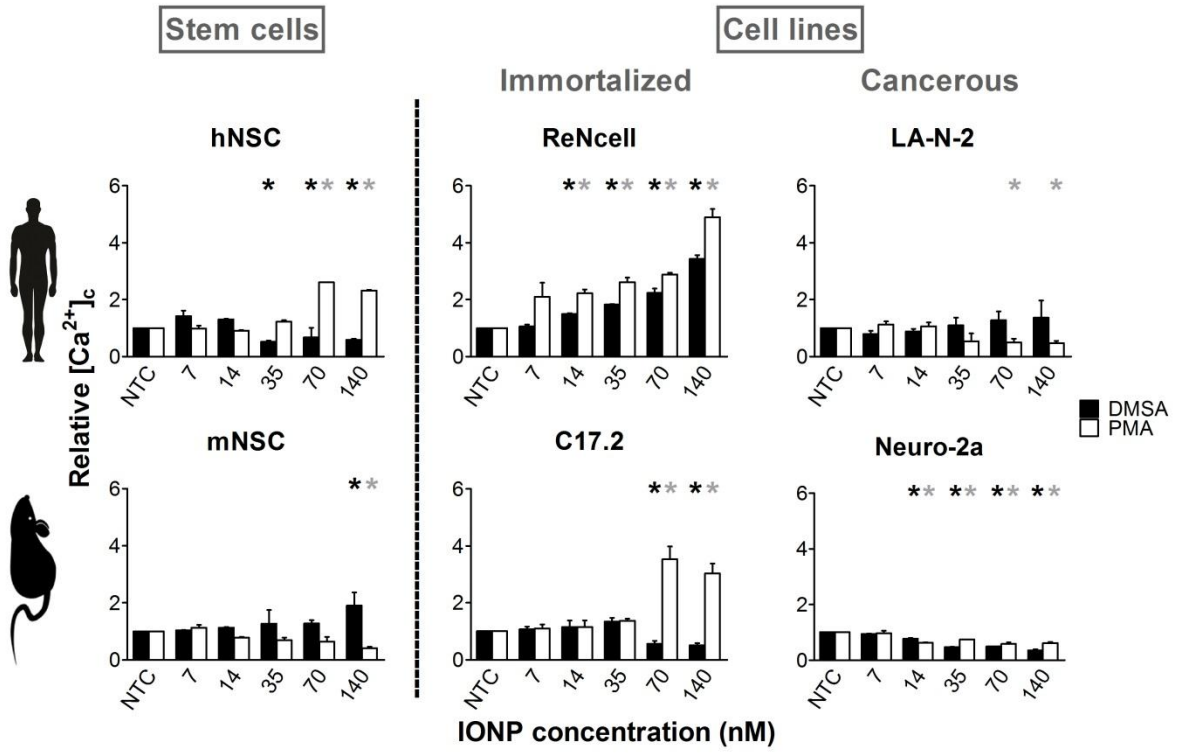

Figure 4: Increased or declined $[Ca^{2+}]_c$ by IONPs.

The cytosolic free calcium concentration ($[Ca^{2+}]_c$) was visualized with Rhod-2 AM following 24 hours exposure to DMSA-IONPs (black bars) and PMA-IONPs (white bars). Grey and black * represent significant alterations when compared to the untreated control (* $p < 0.05$) induced by respectively IONP-PMA and DMSA-IONPs. (NTC = not treated control)

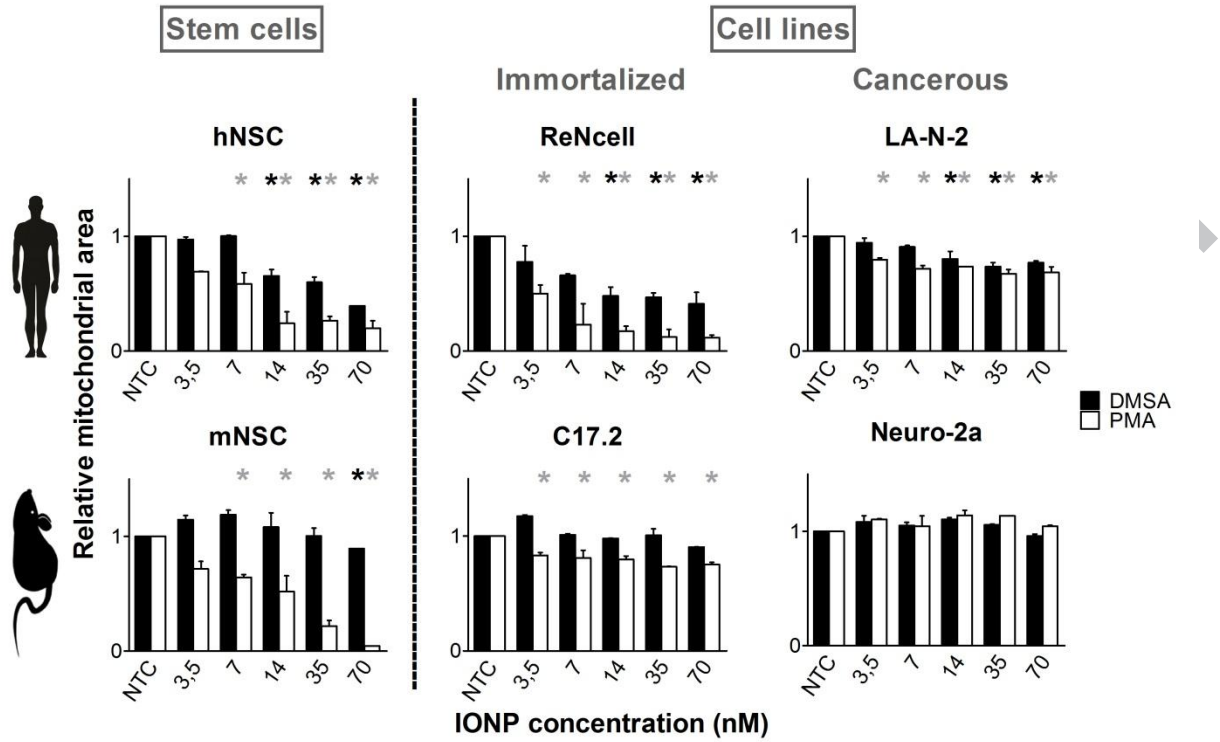

Figure 5: Mitochondria are more severely affected in the human cell types.

DMSA-IONP (black bars) and PMA-IONP (white bars) induced effects on mitochondrial homeostasis in terms of the relative mitochondrial area as visualized with Mitotracker® CMX-ROS. Statistical significance with regard to the untreated control is indicated when appropriate (* $p < 0.05$), in black for significant effects evoked by IONP-DMSA and in gray for the PMA-coated IONP. (NTC = not treated control)

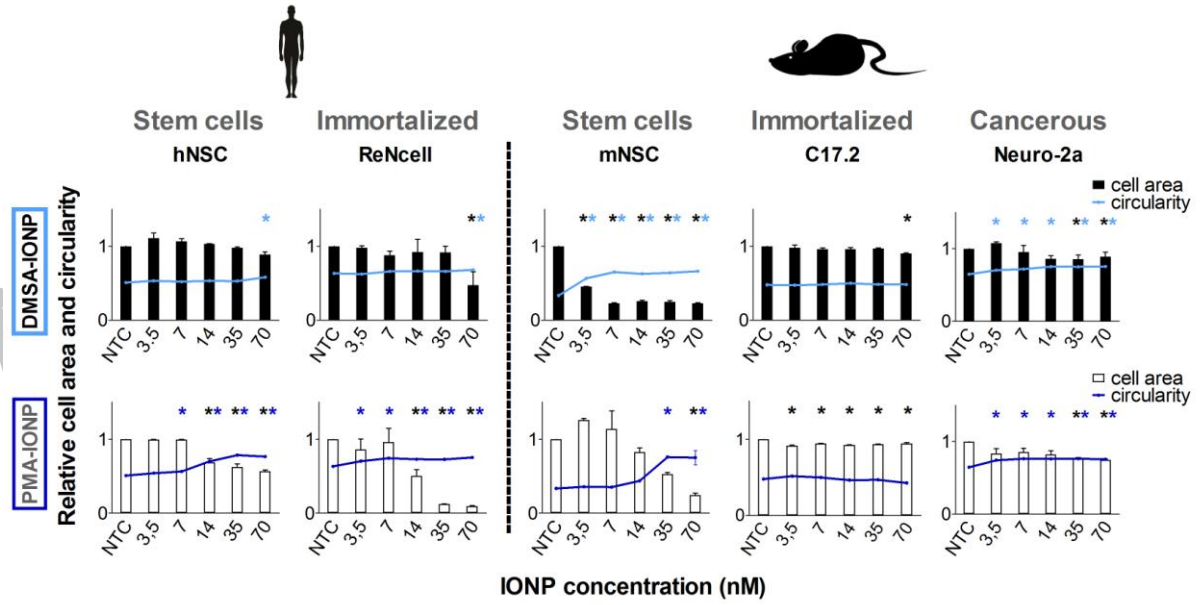

Figure 6: DMSA-IONPs have a minor impact on cell morphology.

The effect on cell morphology of 24 hours exposure to DMSA-IONPs (top row) and PMA-IONPs (lower row) represented as changes in relative cell area (black bars) and cell circularity

(blue lines). In general cell circularity is a more sensitive parameter and DMSA-IONPs induce least severe effects. Statistical significance with regard to the untreated control is indicated when appropriate in the corresponding color, black for cell area and blue for circularity (* $p < 0.05$). (NTC = not treated control)

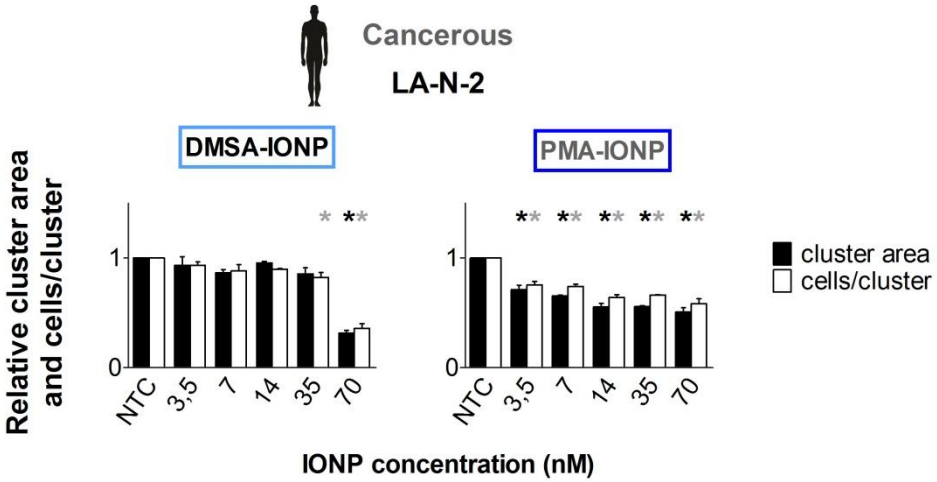

Figure 7: LA-N-2 cell morphology is least affected by DMSA-IONP exposure.
The effect of both IONPs on the LA-N-2 cell line in terms of the total cluster area (black bars) and cells per cluster (white bars). Grey and black * represent significant alterations when compared to the untreated control (* $p < 0.05$) for respectively cluster area and cells per cluster. (NTC = not treated control)

Choose Your Cell Model Wisely: The *In Vitro* Nanoneurotoxicity of Differentially Coated Iron Oxide Nanoparticles for Neural Cell Labeling.

Freya Joris[▲], *Daniel Valdepérez*[†], *Beatriz Pelaz*[†], *Tianqiang Wang*[†], *Shareen H. Doak*[§], *Bella B. Manshian*[◊], *Stefaan J. Soenen*[◊], *Wolfgang J. Parak*[†], *Stefaan C. De Smedt*[▲,1,*], *Koen Raemdonck*[▲,1]

[▲] Lab of General Biochemistry and Physical Pharmacy, Faculty of Pharmaceutical Sciences, Ghent University, Ottergemsesteenweg 460, B-9000 Ghent, Belgium.

[†] Philipps University of Marburg, Department of Physics, Renthof 7, D-35037 Marburg, Germany.

[§] Institute of Life Sciences, Swansea University Medical School, Singleton Park, Swansea, Wales, SA2 8PP, UK.

[◊] Biomedical MRI Unit/MoSAIC, Department of Medicine, KULeuven, Herestraat 49, B-3000 Leuven, Belgium.

[1] The authors contributed equally to this work

* Address correspondence to: stefaan.desmedt@ugent.be

STATEMENT OF SIGNIFICANCE

Inorganic nanoparticle (NP) optimization is chiefly performed *in vitro*. For the optimization of iron oxide (IO)NPs for neural stem cell labeling in the context of regenerative medicine human or rodent neural stem cells, immortalized or cancer cell lines are applied. However, the use of certain cell models can be questioned as they phenotypically differ from the target cell. The impact of the neural cell model on nanosafety remains relatively unexplored. Here we evaluated cell homeostasis upon exposure to PMA- and DMSA-coated IONPs. Of note, the DMSA-IONPs outperformed the PMA-IONPs in each cell type. However, distinct cell type-specific effects were witnessed indicating that nanosafety should be evaluated in a human cell model that represents the target cell as closely as possible.

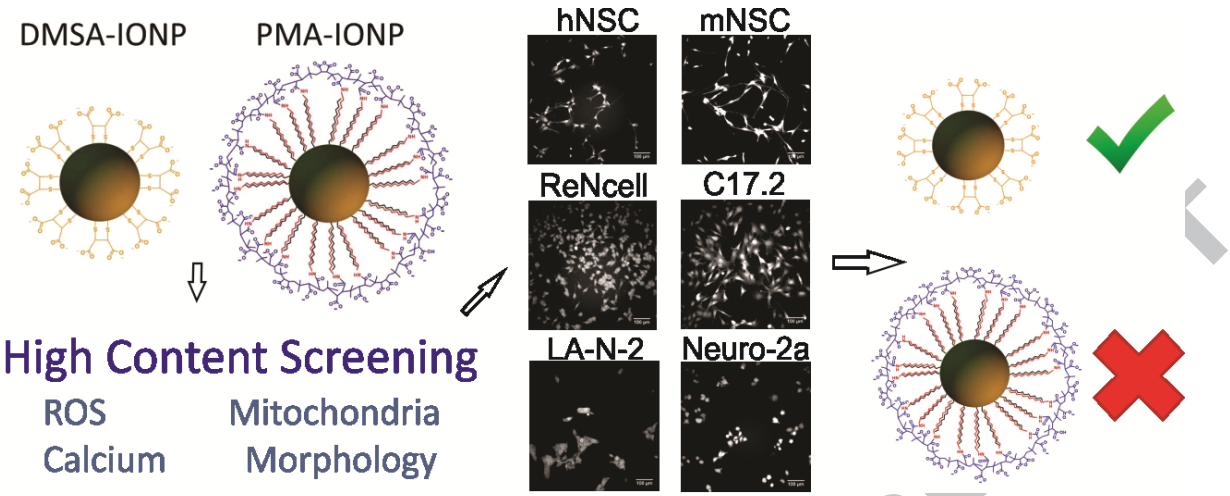

Graphical abstract